The Structure of Amorphous Platinum Disulfide as Studied by Anomalous X-ray Scattering

Masatoshi Saito[1], Makoto Wakeshima[1], Nobuaki Sato[1], Takeo Fujino[1], Yoshio Waseda, Eiichiro Matsubara[2], and K. Thomas Jacob[3]

[1] Institute for Advanced Materials Processing, Tohoku University, Sendai 980-77, Japan
[2] Department of Materials Science and Engineering, Graduate School, Kyoto University, Kyoto 606, Japan
[3] Materials Research Centre and Department of Metallurgy, Indian Institute of Science, Bangalore 560012, India

Z. Naturforsch. **49a**, 1031–1036 (1994); received September 13, 1994

Anomalous X-ray scattering (AXS) has been applied to study the structure of amorphous platinum disulfide, $Pt_{1-x}S_2$, prepared by the precipitation process. The local atomic arrangement in amorphous $Pt_{1-x}S_2$ was determined by the least-squares variational method so as to reproduce the experimental differential interference function at the Pt L_{III} absorption edge by the AXS method as well as the ordinary interference function by Mo $K\alpha$. The structural unit in amorphous $Pt_{1-x}S_2$ is found to be a PtS_6 octahedron, similar to that in crystalline PtS_2. These octahedra share both their corners and edges, while only edge-sharing linkages occur in crystalline PtS_2.

Introduction

Crystalline chalcogenides with a Group IV B to VIII B transition metal (M) are known to have a layered structure in MX_2 and a chain-like structure in stoichiometric MX_3 [1]. These crystalline chalcogenides have many interesting properties, such as charge density waves, intercalation chemistry and superconductivity, arising from their highly anisotropic and low dimensional structure. Amorphous transition metal chalcogenides are formed by precipitation from aqueous or non-aqueous solution at low temperature or by thermal decomposition of thio or seleno salts [2]. They frequently show better catalytic and electrochemical properties than the crystals.

The main purpose of this work is to present new structural information on amorphous platinum disulfide prepared from aqueous solution by applying the anomalous X-ray scattering (AXS) method.

Sample Preparation

Passaretti et al. [3] have prepared amorphous $Pt_{1-x}S_2$ by the reaction of anhydrous hexachloroplatinate with hydrogen sulfide at various temperatures. The reaction time and temperature in this process were found to be critical. If the reaction temperature was too high, the hexachloroplatinate complex decomposed, while if the reaction temperature was too low, the reaction was not completed. In this work, the reaction was carried out in aqueous solution and amorphous platinum sulfide was obtained without such difficulties.

Hexachloroplatinic(IV) acid H_2PtCl_6 was prepared by dissolving platinum in aqua regia. Hydrochronic acid was added to the solution. This solution was evaporated to obtain a syrupy form so as to drive off the nitric acid and any $PtCl_4 \cdot 2\,NOCl$ which may be included. The thick solution was taken up with HCl and the resulting solution reevaporated to a syrup. This process was repeated several times. The residue was then diluted with distilled water. Finely dispersed precipitates of amorphous $Pt_{1-x}S_2$ were produced by passing H_2S gas through this H_2PtCl_6 solution at room temperature. The precipitation was filtered off and extracted with carbon disulfide CS_2 to remove any sulfur that may have been deposited with the products. After extraction, the amorphous $Pt_{1-x}S_2$ powder was carefully dried under vacuum so as to prevent oxidation by air, since it might be pyrophoric.

The ratio of sulfur to platinum in the amorphous sample was determined by thermogravimetric (TG) analysis with a balance using a silica spring. The heating rate was 5 K/min. The thermogravimetric curve is shown in Figure 1. It is seen that the sample starts to decompose at about 473 K and completely decomposed into Pt and S above 773 K. The X-ray powder

Reprint requests to Dr. Masatoshi Saito.

0932-0784 / 94 / 1100-1031 $ 06.00 © – Verlag der Zeitschrift für Naturforschung, D-72027 Tübingen

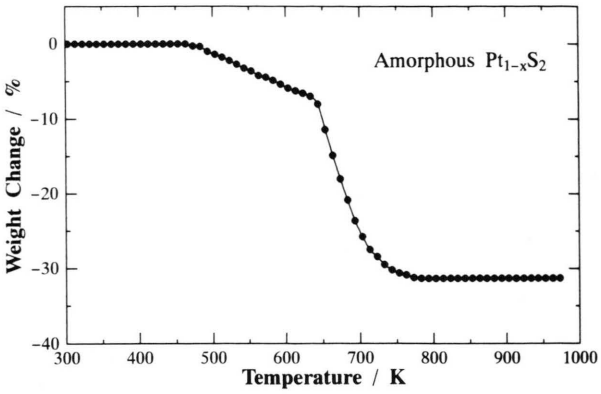

Fig. 1. TG curve measured in air for amorphous $Pt_{1-x}S_2$.

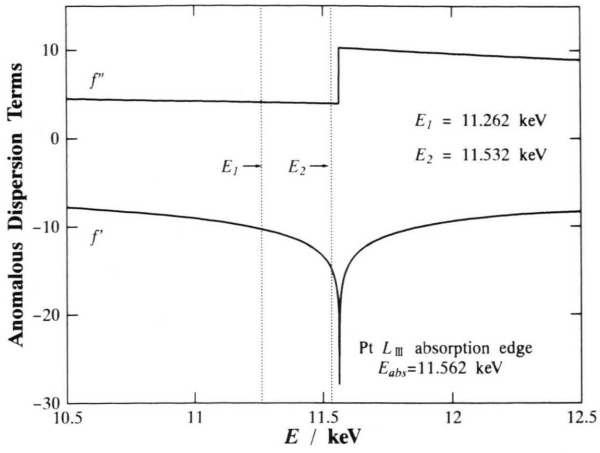

Fig. 2. Theoretical energy dependence of anomalous dispersion terms for Pt near the L_{III} absorption edge, as calculated by Cromer and Lieberman's method.

diffraction pattern of the decomposed product has clearly confirmed the formation of metallic platinum. Assuming that the weight loss detected in this TG analysis is induced by sulfur release, the estimated value of x in the present amorphous $Pt_{1-x}S_2$ sample is 0.22. The mass density of amorphous $Pt_{1-x}S_2$, determined by the Archimedean method with toluene, is 5.7 g/cm^3.

Experimental

The ordinary X-ray scattering measurement was carried out with Mo$K\alpha$ radiation. The AXS measurements were carried out at the beam line 6B in the Photon Factory of the National Laboratory for High-Energy Physics, Tsukuba, Japan. Monochromatic incident X-rays at energies from 4 to 21 keV were obtained with a Si(111) double-crystal monochromator. The sample was mounted on a double-axis diffractometer placed vertically so as to eliminate the polarization effect. The incident beam was monitored by a nitrogen-gas-flow-type ion chamber placed in front of the sample. By using the monitor counts, the number of photons incident on the sample was kept constant. Scattering intensities were measured by a scintillation counter with a pulse height analyzer. After the corrections for air scattering, absorption and polarization, the measured intensity was converted to electron units per atom by the generalized Krogh-Moe-Norman method using the X-ray atomic scattering factors and their anomalous dispersion terms [4]. The Compton scattering was corrected by the tabulated values [5].

Details of the data analysis of the AXS measurements have been given in [6]. Only some essential points are given below. When the energy of the incident X-ray beam is close to the absorption edge E_{abs} of one of the constituent elements, the atomic scattering factor becomes complex due to resonance scattering phenomena and can be expressed in the form $f(Q,E) = f^0(Q) + f'(E) + if''(E)$, where Q and E are the wave vector and the incident X-ray energy, respectively. $f^0(Q)$ corresponds to the normal atomic scattering factor. The terms of $f'(E)$ and $f''(E)$ are the real and imaginary parts of the anomalous dispersion term, which depend upon the energy of the incident X-rays. Figure 2 shows the energy dependence of $f'(E)$ and $f''(E)$ of Pt calculated in the close vicinity of the Pt L_{III} absorption edge (11.562 keV) [7]. When the incident energy is set to an energy below Pt L_{III} absorption edge, the detected variation in intensity $\Delta i_{Pt}(Q)$ is attributed only to a change of the anomalous dispersion terms of Pt, f'_{Pt}. Therefore, the following relation is readily obtained [8]:

$$\Delta i_{Pt}(Q) = \frac{\{I(Q,E_1) - \langle f^2(Q,E_1)\rangle\} - \{I(Q,E_2) - \langle f^2(Q,E_2)\rangle\}}{c_{Pt}\{f'_{Pt}(E_1) - f'_{Pt}(E_2)\}\, W(Q)}$$

$$= \int_0^\infty 4\pi r^2 \sum_k^{\text{elements}} \frac{\mathrm{Re}\{f_k(Q,E_1) + f_k(Q,E_2)\}}{W(Q)} \cdot (\varrho_{Ptk}(r) - \varrho_{0k}) \frac{\sin(Q\,r)}{Q\,r}\,\mathrm{d}r, \qquad (1)$$

$$W(Q) = \sum_{k}^{\text{elements}} c_k \,\mathrm{Re}\,\{f_k(Q, E_1) + f_k(Q, E_2)\},$$

where $E_{abs} > E_2 > E_1$, $I(Q, E_i)$ is the coherent X-ray scattering intensity in electron units per atom, c_k the atomic fraction of the k-element, $\varrho_{Pt\,k}(r)$ the radial density function of the k-element around Pt at a radial distance of r, and $\varrho_{0\,k}$ the average number density of the k-element in the system. "Re" denotes the real part of the values in the brackets. Thus, the environmental radial distribution function (RDF) for Pt is obtained by Fourier transformation of the quantity of $Q\,\Delta i_{Pt}(Q)$ in (1):

$$4\pi r^2 \varrho_{Pt}(r) = 4\pi r^2 \varrho_0 + \frac{2r}{\pi} \int_0^{\infty} Q\,\Delta i_{Pt}(Q) \sin(Q r)\,\mathrm{d}Q, \tag{2}$$

where ϱ_0 is the average number density in the system. Consequently, the environmental structure around Pt is obtained by measuring the energy dependence of the X-ray scattering intensity in the close vicinity of the Pt absorption edge.

Results and Discussion

Figure 3 shows the coherent scattering of amorphous $Pt_{1-x}S_2$ in electron units per atom obtained by the ordinary X-ray scattering measurement with Mo$K\alpha$ radiation. This profile is typical for an amorphous structure except for the increase in the small-angle X-ray scattering. This increase in intensity below $Q = 15\ \mathrm{nm}^{-1}$ is a known spurious effect due to the sensing of the primary beam by a detector. The effect has been checked by placing an additional slit systeme which narrows the incident and diffracted beams. Figure 4 shows two intensity profiles measured at incident energies of 11.532 and 11.262 keV. These two energies are 30 and 300 eV below the Pt L_{III} absorption edge (11.562 keV). Theoretical values of the anomalous dispersion terms for Pt and S used in the present work are found to agree well with the experimental ones at the lower energy side of the absorption edge [9]. Figure 4 also gives the intensity difference $\Delta I_{Pt}(Q)$ from which the differential interference function $Q\,\Delta I_{Pt}(Q)$ in (1) is obtained. The environmental RDF for Pt in amorphous $Pt_{1-x}S_2$ is obtained by Fourier transformation, and the result is compared with the ordinary RDF in Figure 5. It may be worth noting that a direct comparison between the two curves is only possible for the values on the abscissa, because different weighting factors are used on the ordinate. The sharp and almost completely isolated first peak at 0.234 nm suggests the presence of a certain chemical short-range order in amorphous $Pt_{1-x}S_2$. The fundamental structural unit of crystalline PtS_2, illustrated in Fig. 6, consists of a Pt atom octahedrally surrounded by six S atoms, and these slightly distorted PtS_6 octahedra share their edges so as to form a layered structure. S atoms belonging to adjacent layers are held together by Van der Waals forces, while there is a strong mixed covalent-ionic bond between nearest neighboring Pt and S pairs. The vertical lines in Fig. 5 indicate the peak positions expected in this crystal form [10]. Taking this informa-

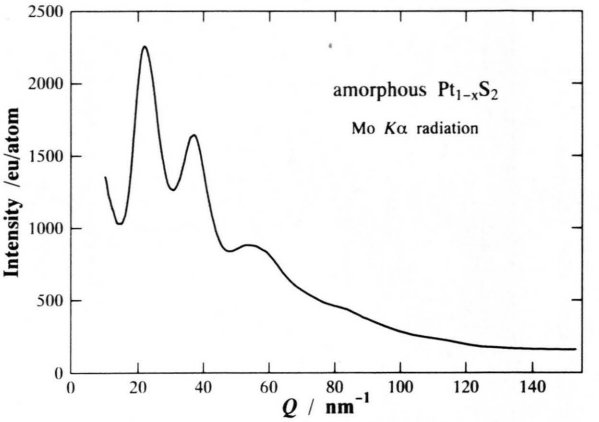

Fig. 3. Scattering intensity profile from amorphous $Pt_{1-x}S_2$ with Mo$K\alpha$ radiation.

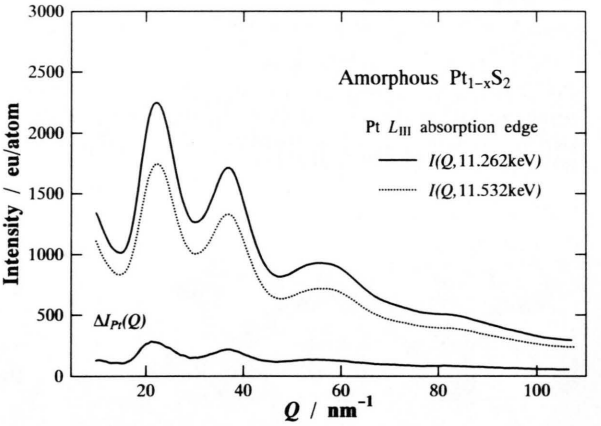

Fig. 4. Differential intensity profile of amorphous $Pt_{1-x}S_2$ (bottom) obtained from the intensity profiles (top) measured at incident energies of 11.262 and 11.532 keV, which correspond to energies of 300 and 30 eV below the Pt L_{III} absorption edge.

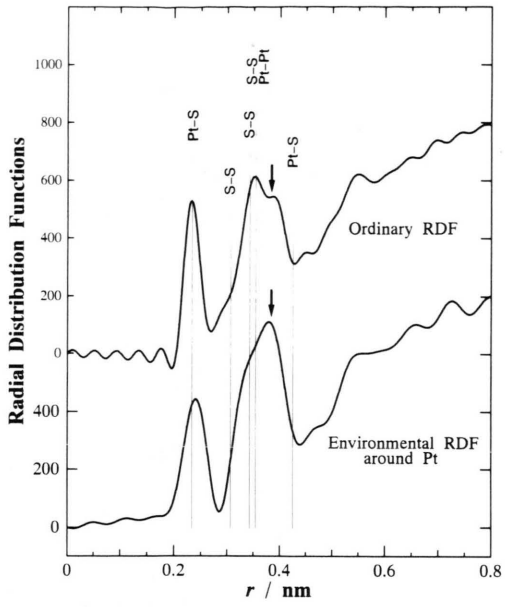

Fig. 5. Ordinary radial distribution function (RDF) and environmental RDF determined from the differential intensity profiles in Figure 4. Vertical lines indicate the peak positions found in crystalline PtS_2 of CdI_2-type structure.

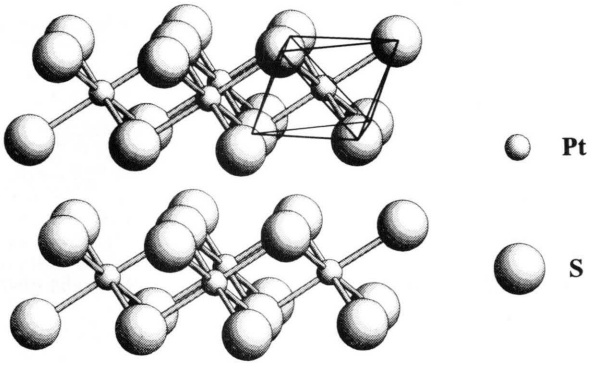

Fig. 6. Schematic diagram for the fundamental structural unit in crystalline PtS_2 composed of a Pt atoms with six S atoms sharing the edges of slightly distorted octahedron.

tion, the first peak of the RDFs in Fig. 5 is attributed to Pt–S pairs. Then, the coordination number of the nearest neighboring S atoms around Pt is estimated to be 5.5. Therefore, it is plausible that a fundamental unit structure similar to that in the PtS_2 crystal prevails also in the amorphous state.

The structural parameters such as atomic distances and coordination numbers of amorphous materials have been successfully determined by the least squares variational method originally proposed by Narten and Levy [11]. According to Narten and Levy, the interference function is given by

$$Q\,i(Q) = \sum_{j=1}^{N} \sum_{k} c_j \frac{f_j f_k}{\langle f \rangle^2} \frac{N_{jk}}{r_{jk}} \exp(-b_{jk} Q^2) \sin(Q r_{jk}) + \sum_{\alpha=1}^{N} \sum_{\beta=1}^{N} \frac{c_\alpha c_\beta f_\alpha f_\beta}{\langle f \rangle^2} 4\pi \varrho_0 \exp(-b_{\alpha\beta} Q^2) \cdot \frac{Q R_{\alpha\beta} \cos(Q R_{\alpha\beta}) - \sin(Q R_{\alpha\beta})}{Q^2}, \quad (3)$$

where N_{jk} is the number of type-k atoms around any type-j atom at the distance of r_{jk} and the value of b_{jk} is the mean square variation. The quantities of $R_{\alpha\beta}$ and $b_{\alpha\beta}$ correspond to the mean size and the variance of the boundary region. The first and second terms on the right hand side of (3) represent a discrete Gaussian-like distribution in the neighboring region and a continuous distribution with an average number density at long distances, respectively. The distance and coordination number for near-neighbors are refined by the least-squares calculation of (3) so as to reproduce two independent experimental interference functions by the AXS method for Pt and by the ordinary diffraction with Mo$K\alpha$ radiation [12]. It should be kept in mind that this method is not a unique mathematical procedure, but the structural parameters in the near neighbor region can be quantified with a much higher reliability in a sense of the necessary condition at best. The non-linear least-squares program developed by Levy et al. [13] was slightly modified for convenience of the present analysis.

The least-squares variational method is usually carried out by iteration with the local structural information in a crystal as starting parameters. In the present case however, a difficulty appears for the peak at about 0.38 nm which is not recognized in crystalline PtS_2, as shown in Figure 5. Since this peak is observed in both environmental and ordinary RDFs and referring to the arrangement of the octahedral units, the peak at about 0.38 nm is hardly explained by Pt–S pairs. Thus, this peak should be attributed to the correlation of Pt–Pt pairs. The PtS_6 octahedra in crystalline PtS_2 are connected with the adjacent octahedra by edge sharing, as schematically shown in Figure 7(a). The coordination number between the nearest neighboring Pt atoms is 6 at an average distance of 0.354 nm in crystalline PtS_2. When platinum disulfide compounds are prepared from aqueous solu-

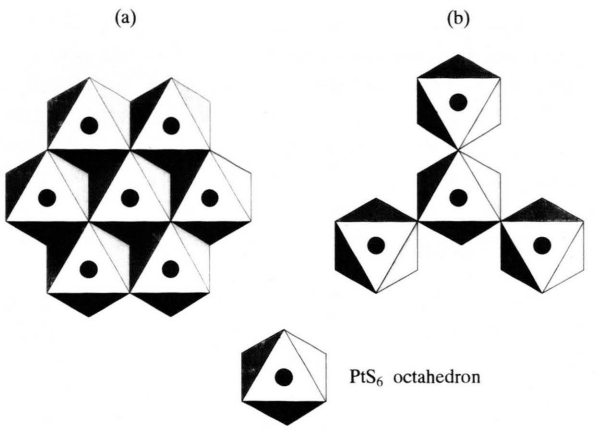

Fig. 7. Schematic diagram of the near neighbor atomic configurations of the PtS_6 octahedral units; (a) edge-sharing linkage, (b) corner-sharing linkage.

tion at relatively low temperature, faulty linkages among some octahedral units might occur. In other words, amorphous platinum disulfide likely contains a large amount of faults in the linkage of the octahedra. The distance observed at about 0.38 nm allocating to the Pt–Pt correlation in the amorphous state enables us to suggest a corner sharing linkage between the octahedra, as shown in Figure 7(b). The maximum coordination number of Pt–Pt pairs is 3 for this linkage. It is apparent that the chemical composition PtS_4 is suggested when the PtS_6 octahedra are everywhere connected with the corner-sharing linkage. Thus, a calculation by least-squares variational fitting was carried out with starting parameters recognized in the crystalline structure and Pt–Pt pairs at about 0.38 nm. The resultant parameters are summarized in Table 1 together with those of the crystalline case. The uncertainty was also estimated from the variance-covariance matrix in the non-linear least-squares variational method and it is included in Table 1. The structural parameters listed in Table 1 reproduce both the difference and ordinary interference functions of $Q\,\Delta i_{Pt}(Q)$ and $Q\,i(Q)$, as shown in Figure 8. This agreement is evidence that the present approach basically works very well. It is found in Table 1 that a Pt atom is surrounded with 5.3 S atoms at 0.235 nm in amorphous $Pt_{1-x}S_2$. The atomic distances of the first and third nearest neighboring S–S pairs are estimated to be 0.300 and 0.353 nm, respectively. No significant difference is detected in these structural parameters the crystalline and amorphous states. This indicates

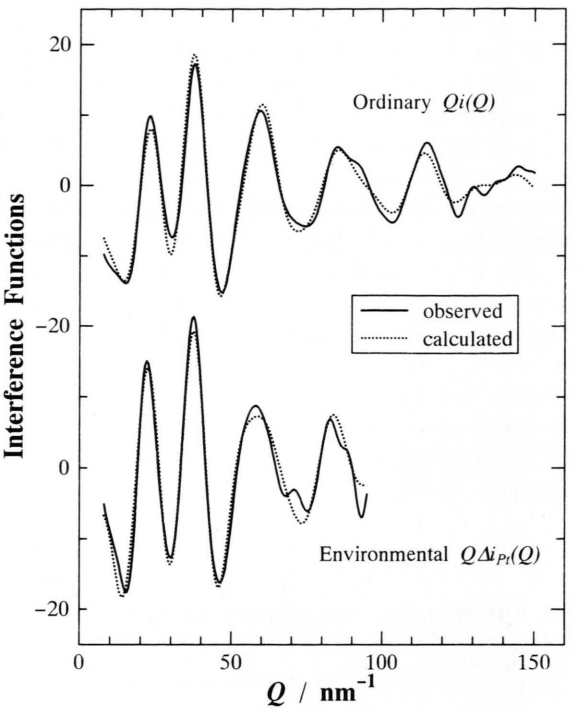

Fig. 8. Interference function of amorphous $Pt_{1-x}S_2$ obtained from the intensity measurement using Mo $K\alpha$ radiation (top) and the environmental interference function $Q\,\Delta i_{Pt}(Q)$ obtained by the AXS measurements at energies close to the Pt L_{III} absorption edge (bottom). Dotted lines denote the calculated values by the least squares variational method.

Table 1. Comparison of near neighbor correlations for amorphous $Pt_{1-x}S_2$ determined by the least squares variation method with those of crystalline PtS_2 of CdI_2-type structure.

Pairs	Crystalline PtS_2 ($P\bar{3}m1$)		Amorphous $Pt_{1-x}S_2$	
	r/nm	N	r/nm	N
Pt–S	0.234	6	0.235±0.002	5.3±0.2
S–S	0.307	3	0.300±0.004	3.4±0.5
S–S	0.343	3	0.310±0.004	3.5±0.5
S–S	0.354	6	0.353±0.004	5.9±0.5
Pt–Pt	0.354	6	0.354±0.002	4.4±0.3
Pt–Pt	–	–	0.398±0.002	1.1±0.2
Pt–S	0.425	6	0.426±0.002	4.1±0.6

that the fundamental structural unit of PtS_6 octahedron remains in amorphous $Pt_{1-x}S_2$. On the other hand, it should be stressed that the structure of amorphous $Pt_{1-x}S_2$ is characterized by an additional correlation of the second nearest neighboring Pt–Pt pairs. The number of the first nearest neighboring Pt–Pt pair is 4.4, which is less than 6.0 in PtS_2 crystal.

The second nearest neighboring Pt–Pt pair at 0.398 nm, which is not present in the PtS_2 crystal, shows a coordination number of 1.1. As mentioned above, the first and second nearest neighboring Pt–Pt pairs correspond to an edge sharing linkage (6 Pt–Pt pairs) and a corner sharing linkage (3 Pt–Pt pairs), respectively. The molar ratio of Pt atoms with the edge-sharing octahedron to those with the corner-sharing one is then 2:1 (= 4.4/6:1.1/3). The chemical composition of the present sample, which includes these two kinds of linkage of octahedra can be roughly estimated as follows. When considering that the edge-sharing and corner-sharing octahedra spatially coexist with the molar ratio of 2 to 1, the average value of the composition leads to $Pt_{0.75}S_2$ ($= PtS_2 + 1/2\ PtS_4)/2$), namely, $x = 0.25$ in $Pt_{1-x}S_2$. This value coindices well will the observed one in the present TG analysis. It is supposed from the structural point of view that the open structure associated with such a deficiency of Pt atoms is probably one of the significant factors in determining the catalytic and electrochemical properties of amorphous $Pt_{1-x}S_2$.

Acknowledgements

The authors would like to express their gratitude to Prof. M. Nomura, Photon Factory, National Laboratory for High-Energy Physics for his kind help on the AXS measurements. This work was supported by the Grant-in-Aid for Scientific Research from the Ministry of Education, Science and Culture of Japan (No. 05 750 591).

[1] F. Hulliger, Structural Chemistry of Layer-Type Phases, ed. F. Levy; D. Reidel Publishing Co., Dordrecht 1976, Holland.
[2] R. R. Chianelli and M. B. Dines, Inorg. Chem. **17,** 2757 (1978).
[3] J. D. Pasaretti, R. B. Kaner, R. Kershaw, and A. Wold, Inorg. Chem. **20,** 501 (1981).
[4] J. A. Ibers and W. C. Hamilton, ed., International Tables for X-ray Crystallography, Vol. IV, Birmingham 1974, Kynoch.
[5] D. T. Cromer and J. B. Mann, J. Chem. Phys. **47,** 1892 (1967).
[6] Y. Waseda, Novel Application of Anomalous X-ray Scattering for Structural Characterization of Disordered Materials, Springer-Verlag, New York 1984.
[7] D. T. Cromer and D. L. Lieberman, J. Chem. Phys. **53,** 1891 (1970).
[8] E. Matsubara, Y. Waseda, M. Mitera, and T. Masumoto, Trans. JIM. **29,** 697 (1988).
[9] Y. Waseda, E. Matsubara, and H. Ohta, High Temp. Mater. Processes **8,** 61 (1988).
[10] R. A. Munson and J. S. Kasper, Inorg. Chem. **8,** 1198 (1969).
[11] A. H. Narten and H. A. Levy, Science **160,** 477 (1969).
[12] E. Matsubara, K. Sugiyama, Y. Waseda, M. Ashizuka, and E. Ishida, J. Mater. Sci. Lett. **9,** 14 (1990).
[13] H. A. Levy, M. D. Danford, and A. H. Narten, ORNL Report No. ORLN-3960 (1966).